Functionalized Bridged Silsesquioxane-based Nanostructured Microspheres: Performance as Novel Drug-delivery Devices in Bone Tissue-related Applications

HERNÁN ESTEBAN ROMEO* AND MARÍA ALEJANDRA FANOVICH
Institute of Materials Science and Technology (INTEMA), University of Mar del Plata and National Research Council (CONICET), J. B. Justo 4302, B7608FDQ, Mar del Plata, Argentina

ABSTRACT: Two kinds of functionalized nanostructured hybrid microspheres, based on the bridged silsesquioxane family, were synthesized by employing the sol–gel method *via* self-assembly of two different organic–inorganic bridged monomers. The architecture reached at molecular level allowed the incorporation of acetylsalicylic acid (ASA) as an anti-inflammatory model drug. The ASA-functionalized microspheres were characterized as delivery devices in simulated body fluid (SBF). The release behaviors of the synthesized microspheres (Fickian or anomalous diffusion mechanisms) were shown to be dependent on the chemical nature of the bridged monomers employed to synthesize the hybrid materials. The functionalized microspheres were proposed as delivery systems into calcium phosphate cements (CPCs), in order to slow down the characteristic drug-delivery kinetics of this kind of bone tissue-related materials. The incorporation of the new functionalized microparticles into the CPCs represented a viable methodology to modify the ASA-release kinetics in comparison to a conventional CPC containing the drug dispersed into the solid phase. The ASA-delivery profiles obtained from the

*Author to whom correspondence should be addressed. E-mail: hromeo@fi.mdp.edu.ar

0885-3282/12/08 0987–26 $10.00/0 DOI: 10.1177/0885328210389503

microsphere-loaded CPCs showed that 40–60% of drug can be released after 2 weeks of testing in SBF. The inclusion of the microspheres into the CPC matrices allowed modification of the release profiles through a mechanism that involved two stages: (1) the diffusion of the drug through the organic–inorganic matrix of the microspheres (according to a Fickian or anomalous diffusion, depending on the nanostructuring) and (2) the subsequent diffusion of the drug through the ceramic matrix of the hardened cements. The release behavior of the composite cements was shown to be dependent on the nanostructuring of the hybrid microspheres, which can be selectively tailored by choosing the desired chemical structure of the bridged precursors employed in the sol–gel synthesis. The obtained results demonstrated the ability of this new class of functionalized hybrid microdevices as delivery systems into calcium phosphate materials with potential bone tissue-related drug-delivery applications.

KEY WORDS: drug-delivery, hybrid materials, microspheres, calcium phosphate cements, composite biomaterials.

INTRODUCTION

In the last years, the incidence of musculoskeletal disorders, such as osteoporosis, osteoarthritis, osteomyelitis, among others, has led to major efforts focused on the pharmacological treatment of these illnesses, employing different drug-delivery devices to sustain the effect of the drug at the specific target site [1–3]. An ideal drug carrier for bone tissue-related applications should be bioactive, which would ensure the ability of the biomaterial to bond to living bone, and resorbable to allow its progressive substitution by newly formed tissue. In addition to these requirements, some advantages are provided if the material is injectable, since it would improve ease of administration, allowing minimally invasive surgical techniques. Considering the mentioned characteristics, these are very well fitted by calcium phosphate cements (CPCs), which have been widely employed as bone-ingrowth materials [4–6]. However, one of the main disadvantages of these systems comes from the rapid release behavior that characterizes CPCs when they are used as drug-delivery devices, leading to large amounts of drug released during the first hours of the setting and hardening processes. For these reasons, one of the most employed strategies to overcome these effects has been the encapsulation of drugs into polymer microparticles, in order to slow down the drug release kinetics into the cement matrix [7]. An applied methodology to control, for instance, bone infections has been the implantation of CPCs loaded with gentamicine sulfate-functionalized polymethylmethacrylate (PMMA) spheres [8], vancomycin-functionalized PCL

microparticles [9], among others, leading to successful results when evaluated in simulated body fluids (SBFs).

Well-defined spherical particles of different nature have also attracted great attention since they have shown to be useful in many applications on advanced technologies, including those related to biosciences field [10]. If a patterned structure can be generated inside these spheres, some new properties which cannot be obtained from simple spheres (for example, stepwise drug release), are expected. There are a number of different polymeric materials that offer the possibility of obtaining ordered structures after polymerization takes place. Among these materials, the bridged silsesquioxane family has been recognized to have an enormous potential as building blocks for various advanced nanostructured devices, including those related to biomedical applications [11]. These silica-based bridged hybrids are obtained *via* sol–gel method, by hydrolysis and condensation of monomers containing an organic bridging group covalently bonded to terminal trialkoxysilyl or trichlorosilyl groups [12,13]. Depending on the nature of the bridge, which could exhibit self-assembling properties, different degrees of organization at molecular level can be achieved during the hydrolytic condensation of the precursors. In this way, the versatility of the sol–gel processing to synthesize nanostructured materials and the possibility of incorporating organic molecules into the resulting hybrid matrix, represent a novel and attractive path to the synthesis of new functionalized organic–inorganic biomaterials with advanced drug-delivery properties.

In a previous study, we reported the sol–gel synthesis and characterization (structural and *in vitro* cytotoxicity characterization) of two different kinds of hybrid microspheres of bridged silsesquioxanes functionalized with acetylsalicylic acid (ASA), employed as anti-inflammatory model drug [14]. The developed method allowed synthesizing monodisperse functionalized microspheres with different nanostructuring at molecular level, which depended on the molecular structure of the employed bridged precursors. The microspheres were demonstrated to be noncytotoxic, showing the ability to retain ASA *via* hydrogen bonds with the organic groups present in the bridges of the precursors.

In this study, we have evaluated the behavior of these new functionalized organic–inorganic microspheres as novel drug-delivery systems in SBF. In addition, on the basis of the drawbacks related to calcium phosphate bone cements, these microspheres were employed as a second phase into a cement matrix, aiming at slowing down the characteristic ASA-release kinetics of this kind of calcium phosphate systems.

MATERIALS AND METHODS

Synthesis of Functionalized Hybrid Microspheres

Glycidoxypropyl(trimethoxysilane) (GPMS, Dow Corning, 99%, density at 20°C = 1.07 g/mL), cyclohexylamine (CA, Merck, 99%, density at 20°C = 0.87 g/mL), dodecylamine (DA, Fluka, 98%, density at 20°C = 0.80 g/mL), formic acid (FA, Cicarelli, 88%, density at 20°C = 1.20 g/mL), ASA (Parafarm, 100%), tetrahydrofuran (THF, Cicarelli, 99%, density at 20°C = 0.89 g/mL), and *n*-hexane (*n*-Hex, Sintorgan, 99%, density at 20°C = 0.66 g/mL), were used without further purification.

Two different precursors of the hybrid microspheres were synthesized from GPMS and two primary aliphatic amines (DA and CA). The stoichiometric reaction between GPMS (2 moles) and the employed amines (1 mole) was selected in order to synthesize bridged precursors containing different organic groups pendant from the organic bridges (alkyl chain or cyclohexyl fragment; see Table 1). Details of the syntheses and characterization of the bridged monomers were described elsewhere [15,16].

The preparation of the functionalized hybrid microspheres was accomplished *via* hydrolytic condensation of the previously synthesized bridged precursors, employing a mixture of THF/*n*-Hex (1 : 2 volumetric blend) as a reaction medium. An aqueous solution of FA was used as catalyst (molar ratios: FA/GPMS = 3 and H_2O/GPMS = 1.05). ASA was used as a model drug to be incorporated into the microspheres during the hydrolytic condensation of the bridged monomers. The addition of the drug was performed by dissolving it in the THF/*n*-Hex mixture, employing a molar ratio ASA/GPMS = 0.5. The FA solution was added dropwise to each system with continuous application of ultrasonic irradiation. The processes were ended when a white suspension appeared in the reaction medium. The obtained suspensions were filtered and the remaining solvent evaporated at 80°C. The resulting powders were placed in a Petri dish and heated in an oven at 110°C for 3 h. The final products (fine yellow glassy powders) were named *GDA* (*G*PMS–*D*A–*A*SA) and *GCA* (*G*PMS–*C*A–*A*SA), depending on the bridged precursor employed in the synthesis. The synthesized microspheres, GDA and GCA, incorporated 13 and 18 wt% of ASA, respectively. Details of the syntheses and characterization of both kinds of hybrid microspheres were described elsewhere [14].

The GDA microspheres evidenced a nanostructuring at molecular level (as determined by small angle X-ray scattering (SAXS) analysis), which led to the formation of cavities consisting of a bilayer

arrangement composed of a tail-to-tail association of dodecyl chains with all trans conformations [14]. On the other hand, the GCA hybrid microspheres were shown to be composed of molecular cavities organized in a two-dimensional hexagonal structure [14].

These two kinds of nanostructured functionalized microspheres were characterized and tested as ASA-delivery systems in simulated physiological conditions. Table 1 summarizes some morphological and structural characteristics of GDA and GCA hybrid microspheres.

Preparation of Calcium Phosphate Cements Containing Functionalized Hybrid Microspheres

The employed cement matrices were based on an equimolar mixture of tetracalcium phosphate (TTCP) and dicalcium phosphate

Table 1. Morphological and structural characteristics of the functionalized hybrid microspheres.

Microsphere system	Mean size (μm)	ASA content (wt%)	Bridged precursor	Nanostructuring
GCA	5.5 ± 0.8	18	Cyclohexyl group pendant from the organic bridge [a]	Two-dimensional hexagonal structure [b]
GDA	4.8 ± 0.2	13	Dodecyl chain pendant from the organic bridge [c]	Tail-to-tail association of dodecyl chains [d]

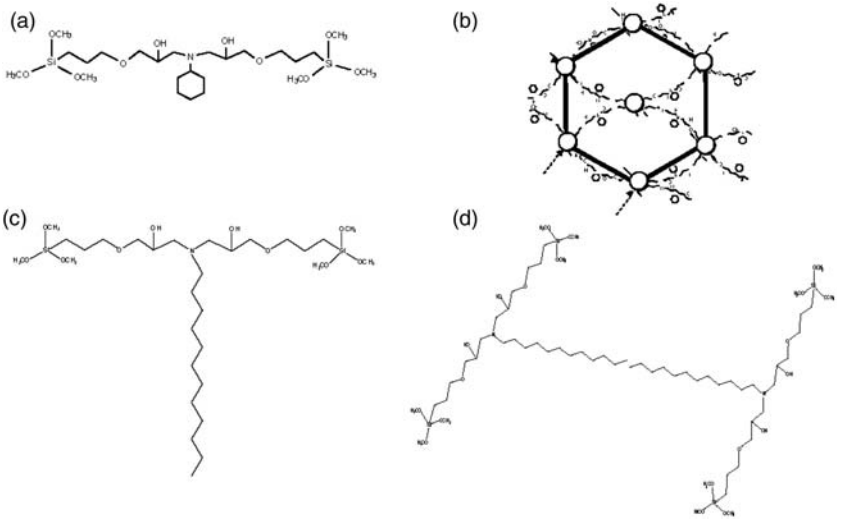

anhydrous (DCPA). Commercially available DCPA from Sigma-Aldrich (99% purity) was used as received. The synthesis of TTCP from reagent-grade $CaCO_3$ (Mallinckrodt, P.A. A.C.S., 99% purity) and $(NH_4)_2HPO_4$ (Merck, P.A. A.C.S., 99% purity) was described elsewhere [17]. A 10 wt% of microspheres (GDA or GCA) was incorporated into the solid phase of each formulation. An aqueous solution of a setting accelerant (5% volume fraction) was employed as the liquid phase of the cement systems [18].

The samples were prepared by mixing 1.3 g of cement powder (TTCP + DCPA + functionalized microspheres: GDA or GCA) with the required amount of the liquid phase to obtain workable pastes. Once obtained, the pastes were placed in polystyrene molds ($1.14 \times 0.50\,cm^2$ in diameter and height, respectively) and stored in a 100% relative humidity incubator at $37 \pm 1^{\circ}C$ for 24 h. Finally, the hardened samples were removed from the molds and polished by a fine abrasive paper. The final dimensions of the polished cement bodies were $1.138 \times 0.30\,cm^2$ in diameter and height, respectively. The prepared cements were named CPC–GDA and CPC–GCA, depending on the nature of the incorporated microspheres.

These two microsphere-loaded bone cements were characterized as ASA carriers and tested as delivery devices in simulated physiological conditions. A cement loaded with ASA dispersed into the solid phase (named CPC–Control) was also prepared and used as a reference material. Table 2 summarizes the cement formulations employed as ASA-delivery devices.

In vitro ASA-Release Behavior of Functionalized Hybrid Microspheres and Calcium Phosphate Composite Cements

An *in vitro* elution method was employed to evaluate the release behavior of both functionalized microspheres and microsphere-loaded cements.

The GDA and GCA samples were wrapped with cellulose acetate membranes (Gamafil®, pore diameter: 0.22 μm) and then immersed in 20 mL of SBF solution. The systems were continuously stirred (90 rpm) at $37 \pm 1^{\circ}C$ for 2 weeks. Different amounts of each type of microspheres (154 mg of GDA and 111 mg of GCA) were employed to conduct the release experiments, in order to work with the same amount of ASA (20 mg) in each test.

The obtained hardened cements (CPC–Control, CPC–GDA, and CPC–GCA) were also immersed in SBF (20 mL) at $37 \pm 1^{\circ}C$ under constant stirring of the systems (90 rpm) for 2 weeks. Cement bodies containing 20 mg of ASA were employed in each case.

Table 2. Compositions of the bone cements employed as ASA-delivery devices.

Cement	Schematic representation	Mass of TTCP/DCPA equimolar mixture (g)	Mass of microspheres (g)	Microspheres (wt%)	Total amount of ASA (mg)	mg ASA/g cement
CPC–Control	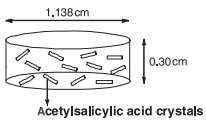	0.980	0	0	20	20
CPC–GCA	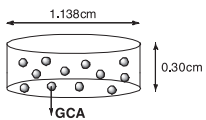	1.000	0.111	10	20	18
CPC–GDA	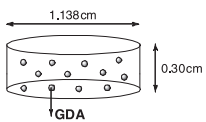	1.384	0.154	10	20	13

In all release experiments, either those accomplished from the functionalized microspheres and calcium phosphate composite cements, aliquots of each solution (3 mL) were collected at predetermined times and replaced with an equivalent volume of fresh SBF solution. Drug concentrations were spectrophotometrically analyzed by means of an Agilent 8453 UV spectrophotometer (diode arrangement) at 224 nm, employing the SBF solution as a reference. The calibration curve was made for the complete set of measurements, displaying a correlation coefficient of 0.99986. All the release tests were carried out in triplicate. The ASA-released percentage (cumulative amount) was finally plotted as a function of time.

The SBF solution employed in all cases (buffered with THAM, pH = 7.25) was prepared according to the following composition: 142.0 mM Na^+, 5.0 mM K^+, 1.5 mM Mg^{2+}, 2.5 mM Ca^{2+}, 147.8 mM Cl^-, 4.2 mM HCO_3^-, 1.0 mM HPO_4^{2-}, and 0.5 mM SO_4^{2-} [19].

Characterization Techniques

Fourier transformed infrared (FTIR) spectra were recorded on the functionalized microspheres with a Genesis II-Mattson device in the absorbance mode, in the range 400–4000 cm^{-1} with a resolution of 2 cm^{-1}. Spectra were obtained using pellets of the samples with KBr.

Morphologies of both functionalized microspheres and cement bodies were observed by scanning electron microscopy (SEM), employing a Jeol JXA-8600 microscope after coating the samples with a thin gold layer.

Initial and final setting times of the cement pastes were determined with Gillmore needles according to the ASTM standard C266-99. The setting times, obtained in triplicate, were expressed as mean ± standard error of the mean. Statistical analysis was performed on the experimental data by means of a Student's *t*-test.

X-ray diffraction (XRD) analyses were performed on hardened CPCs, employing a Philips 1830/00 diffractometer with Fe-filtered Co Kα radiation ($\lambda = 1.79026$ Å). The electrical voltage and current were 40 kV and 30 mA, respectively. Data were collected for 2θ ranging between 10° and 70° with a step size of 1°/min.

RESULTS AND DISCUSSION

Physicochemical Characterization of Functionalized Hybrid Microspheres and Composite Bone Cements

Hybrid Microspheres

SEM images corresponding to GCA functionalized microparticles are shown in Figure 1. Individual microspheres were observed. A mean

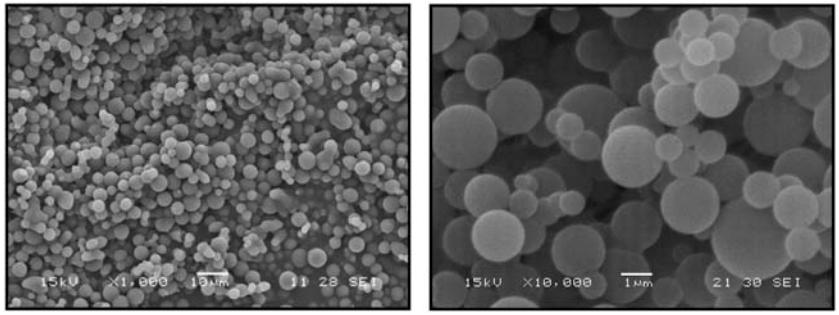

Figure 1. SEM images corresponding to GCA microspheres.

particle size of $5.5 \pm 0.8\,\mu m$, was obtained by image analysis. The microspheres showed a smooth surface without any apparent microporosity. The GDA system exhibited a similar morphology and appearance, showing a mean particle size of $4.8 \pm 0.2\,\mu m$.

Figure 2 depicts the FTIR spectra corresponding to both kinds of microspheres. The spectra showed the characteristic bands corresponding to Si–O–Si (1040 and 1120–1130 cm^{-1}) and unreacted Si–OH (910 cm^{-1}) groups [20]. The broad band located at 3400 cm^{-1} was attributed to C–OH groups (present in the organic bridges of the hybrid materials), including the unreacted fraction of Si–OH groups. Characteristic peaks of ASA were present at 1300 cm^{-1} (H-bonded C–OH of the carboxylic acid), 1600 cm^{-1} (aromatic ring), and 1740 cm^{-1} (carbonyl group of the ester group) [20]. The absence of bands in the region 2500–2700 cm^{-1} indicated that there is no dimerization of carboxylic acids, meaning that ASA was dispersed into the materials forming H-bonds with affine groups of the organic–inorganic hybrid microspheres (tertiary amine, OH, and ether groups) [20].

Composite Bone Cements

Table 3 depicts the initial and final setting times of the prepared cement pastes. According to the obtained results, the composite cements (containing functionalized microspheres) showed shorter setting times in comparison with the CPC–Control cement. The statistical analysis showed no differences on initial ($\sim$12 min) and final ($\sim$20 min) setting times for CPC–GCA and CPC–GDA samples. On the other hand, the CPC–Control cement showed the longest initial and final times (17 and 27 min, respectively), which demonstrated that the dispersion of ASA

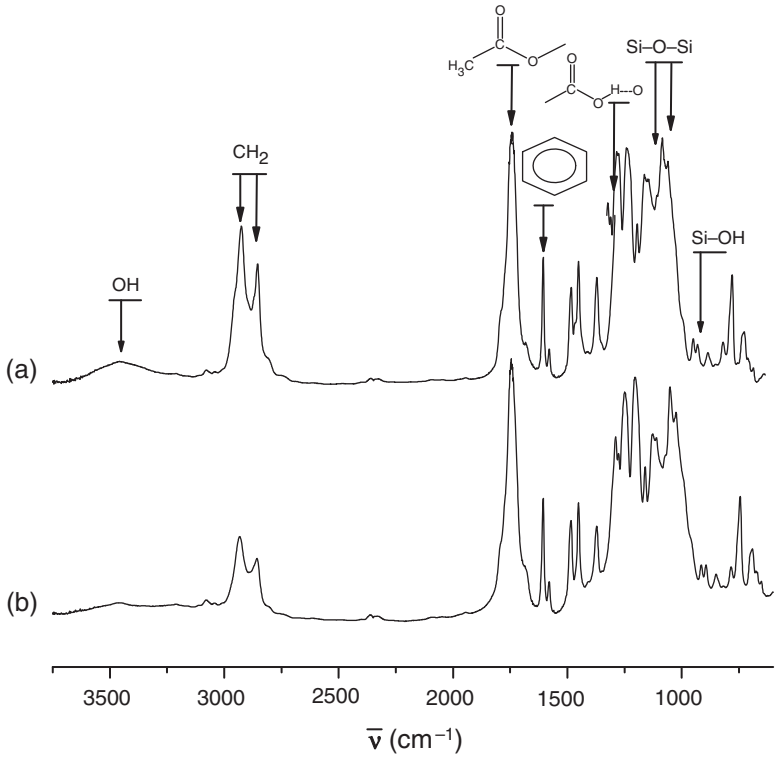

Figure 2. FTIR spectra corresponding to: (a) GDA and (b) GCA.

Table 3. Setting times measured for the prepared cements.

	Setting times (min)	
Cement	Initial	Final
CPC–Control	17 ± 1	27 ± 1
CPC–GCA	11 ± 2	19 ± 1
CPC–GDA	13 ± 1	20 ± 3

into the calcium phosphate matrix effectively modified the physicochemical properties of the system. This effect has been already reported for different active agents employed in CPC formulations [21]. According to this publication, the presence of antibiotics or anti-inflammatory agents in combination with calcium phosphates modifies not only the mechanical properties of the cements, but the setting times

of the pastes as well. Antibiotics, anti-inflammatory agents and other drugs have been demonstrated to increase the setting times, while the mechanical properties are remarkably worsened. These effects have been commonly attributed to the chemical interaction of the drug with the calcium phosphate reactants, which leads to the modification of the dissolution–precipitation kinetics of the calcium phosphates and consequently to changes on the measured setting times.

On this basis, the longer setting times measured for the CPC–Control cement could be attributed to the interaction between ASA molecules and calcium phosphate reactants (TTCP and DCPA). In particular, the formation of complex systems between ASA molecules and Ca^{2+} ions would lead to lengthening of the hydroxyapatite formation time and consequently to the longer setting times measured for this sample. A similar effect was reported for a bone cement based on tricalcium phosphate (α-TCP), containing salicylic acid dispersed into the solid phase [22]. However, the incorporation of functionalized microspheres into the cement matrices allowed us to obtain composite cements containing ASA without modifying the measured setting times of the pastes. This effect can be inferred from the data depict in Table 3.

Figure 3 shows the XRD diffractograms corresponding to the prepared cements. All samples showed the formation of low-crystallinity hydroxyapatite as the main phase, as well as the presence of TTCP and DCPA phases which remained unreacted after 24 h hardening. However, the CPC–Control cement exhibited a lower conversion to hydroxyapatite in comparison to the composite cement systems, as determined from the lower intensity corresponding to the hydroxyapatite patterns and from the higher intensity corresponding to the TTCP and DCPA patterns.

These results, in addition to those obtained from the setting times, demonstrated that the presence of ASA dispersed into the cement matrix interferes with the setting mechanisms that lead to the hardening of the cement systems. However, the incorporation of ASA *via* hybrid microspheres represented a viable and effective alternative to include the drug into the calcium phosphate materials without modifying the physicochemical properties of the cements. SEM micrographs corresponding to the prepared cements clearly revealed an increasing porosity as the systems were loaded with the functionalized microspheres. In both cases (CPC–GCA and CPC–GDA), a more porous microstructure was observed in comparison with that developed for the CPC–Control cement. Figure 4 shows this effect corresponding to the system prepared from GDA microspheres. As a result, the presence of hybrid microspheres into the CPC matrices led to the formation of more

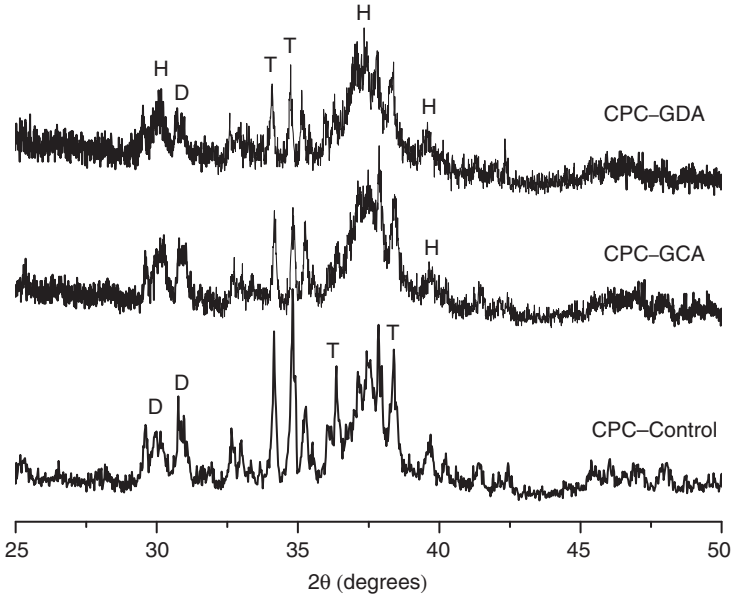

Figure 3. XRD diffractograms corresponding to the prepared calcium phosphate cements after 24 h hardening at $37 \pm 1^{\circ}C$ (100% relative humidity). References: H (hydroxyapatite), T (tetracalcium phosphate), and D (dicalcium phosphate anhydrous).

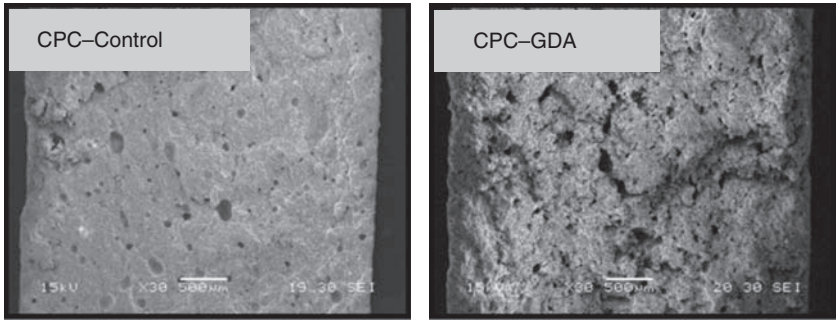

Figure 4. SEM images corresponding to CPC–Control and CPC–GDA cements.

porous cement bodies with the presence of interconnected paths throughout the whole cement samples.

Figure 5 depicts different microstructural aspects developed in CPC–GDA cement after 24 h hardening at $37 \pm 1^{\circ}C$ (100% relative humidity). Figure 5(a) shows the formation of hydroxyapatite

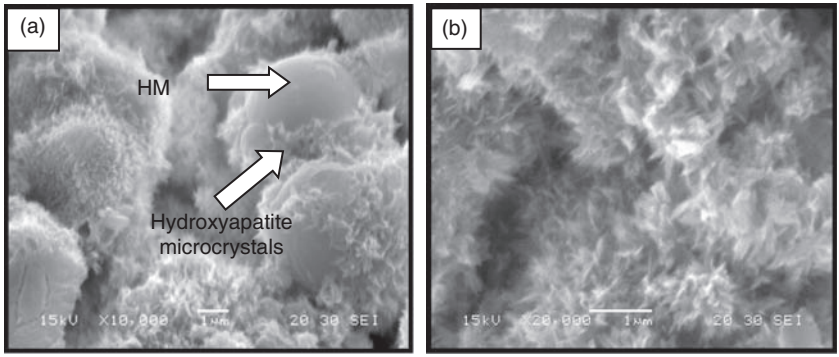

Figure 5. Microstructural aspects developed in CPC–GDA cement. Reference: HM (hybrid microsphere).

microcrystals on the surface of the functionalized microspheres. This observation demonstrated that the presence of these microdevices into the cement matrix did not inhibit the hydroxyapatite formation, which agrees with the XRD results (Figure 3). In addition, the precipitation of the apatite phase on the microspheres demonstrated the surface compatibility between the formed microcrystals and the hybrid materials. It has been already reported, and it is well known, that silanol (Si–OH) groups on the surface of glass-type devices and bioactive glasses play an important role on the deposition of hydoxyapatite [23,24]. For this reason, the observed compatibility was attributed to the presence of Si–OH groups on the surfaces of the functionalized microspheres, which would act as nucleation sites for the apatite phase, promoting the precipitation and subsequent growth of the microcrystals (this fact agrees with the FTIR results, from which the presence of unreacted Si–OH groups on GDA and GCA samples was evidenced). Figure 5(b) shows a closer view of the cement microstructure, in which needle-like hydroxyapatite microcrystals are observed.

Analogous results were obtained for the CPC–GCA composite cement.

Evaluation of Functionalized Hybrid Microspheres and Composite Bone Cements as ASA-Delivery Devices

In vitro ASA-Release Behavior of GDA and GCA Microspheres

The release of drugs from any drug-delivery medical device depends on several aspects such as the micro- and nanostructures of the drug-loaded material, the solubility of the drug in the physiological medium, the bond

nature between the drug and the matrix in which it is retained, the drug concentration, as well as the matrix degradation mechanism, if any. Many systems are characterized for controlling the release behavior by drug diffusion through the matrix (if this matrix is not biodegraded) while other devices make it by degradation of the drug-containing material. However, regardless of the operating mechanism involved, if we are able to develop systems organized at molecular level, different release behaviors and properties (which cannot be obtained from nonstructured materials) could be expected.

Figure 6 shows the ASA-release profiles corresponding to the synthesized microspheres. During the first 4 h, the GDA microspheres showed a faster release kinetics (releasing ~18% of the total drug amount) in comparison to the GCA system (9% released). The same tendency was observed up to the end of the delivery test. After 2 weeks, the GDA microspheres showed a cumulative drug release of 99%, while their counterparts GCA led to 84% released. The faster release kinetics determined for GDA microspheres could be attributed not only to their smaller size (4.8 μm) in comparison to GCA (5.5 μm), but also to the existence of different ASA transport mechanisms through the organic–inorganic hybrid matrices for each material (depending on the characteristic nanostructuring, see Table 1).

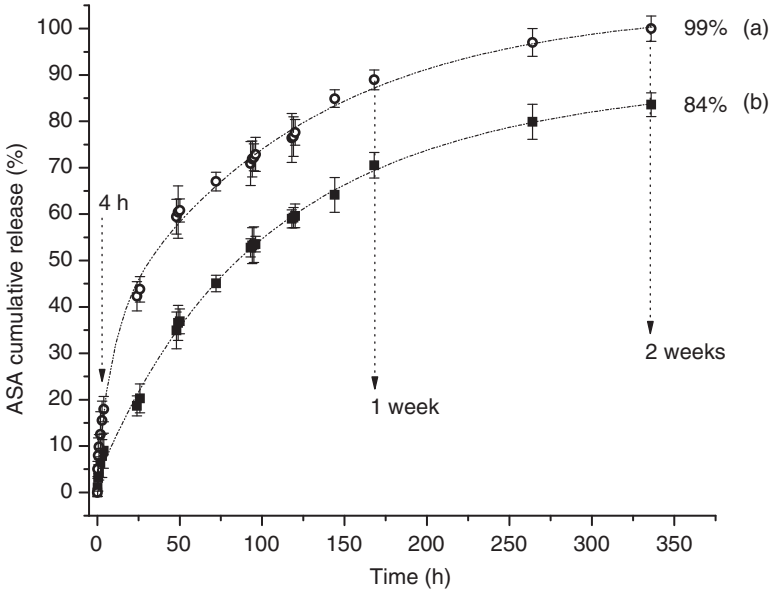

Figure 6. ASA-release profiles corresponding to: (a) GDA and (b) GCA.

In the last 20 years, modeling of controlled drug release from polymeric devices has been the subject of considerable research, most of the employed models being based on particular solutions of the Fickian diffusion equation. However, in the pharmaceutical field, several other expressions have been also found to be useful for the analysis of drugs, for instance, the Higuchi model [25]. In 1984, Sinclair and Peppas [26] proposed a new empirical, exponential expression which related the fractional release of drug to the release time, in order to simplify the analysis of controlled release data from polymeric devices of varying geometry. It was determined, from this equation, that a Fickian diffusional release from a thin film is characterized by an initial $t^{1/2}$ time dependence of the drug release, the time approximation being valid for the first 60% of the total released drug. In addition to this diffusional behavior, a second limiting case could be mentioned where the drug release rate is independent of time (zero-order kinetics). Many situations of release processes fall between these two limiting cases, and they can be represented by coupling of a Fickian and non-Fickian mechanism. In this way, a new generalized expression was proposed by Ritger and Peppas [27] for modeling the experimental data, which can be represented as:

$$M_t/M_\infty = kt^n \tag{1}$$

where M_t/M_∞ is the fractional solute release, t the release time, k a constant incorporating characteristics of the macromolecular network system and the drug, and n is called 'diffusional exponent', which is indicative of the drug transport mechanism. This empirical equation represents an extension of the short-time solutions for Fickian and non-Fickian diffusional release from *thin films*. However, Ritger and Peppas demonstrated that this expression can also be employed for modeling release data from devices with diverse geometry, by defining new diffusional limits of the *diffusional exponent* (depending on geometry). According to the analysis accomplished by these authors, the relationship between the diffusional exponent and the corresponding release mechanism is clearly dependent on the device geometry. In the particular case of drug release from nonswellable spherical devices, the Fickian diffusion is defined by Equation (1) with $n = 0.43$ [27]. Table 4 shows the relationship between the diffusional exponent values and the release mechanisms corresponding specifically to nonswellable spherical devices.

The experimental ASA-release data obtained from both systems of microspheres (Figure 6) were analyzed to obtain the diffusional

Table 4. Relationship between diffusional exponent values and drug-release mechanisms for nonswellable spherical devices.

Diffusional exponent	Drug release mechanism
$n = 0.43$	Fickian diffusion
$0.43 < n < 1.00$	Anomalous transport (non-Fickian)
$n = 1.00$	Zero-order release

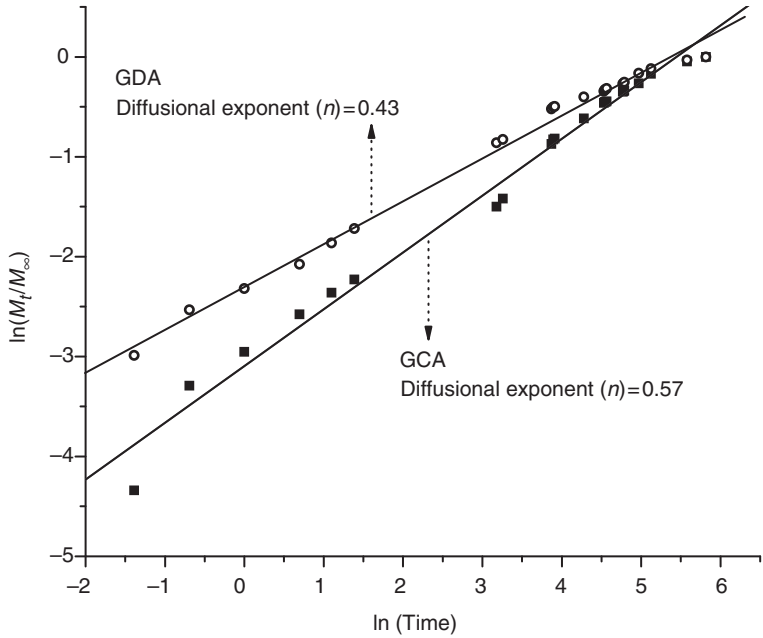

Figure 7. Experimentally obtained diffusional exponents corresponding to the functionalized hybrid microspheres.

exponent values. Figure 7 depicts the $\ln(M_t/M_\infty)$ versus $\ln(t)$ plots for both systems of microspheres. From the slopes of the straight lines, the diffusional exponent values were determined.

According to the obtained results, different ASA transport mechanisms were evidenced depending on the analyzed sample. The GDA microspheres were characterized for a Fickian diffusive transport ($n = 0.43$). On the other hand, the GCA microspheres ($n = 0.57$) evidenced an ASA-anomalous transport. This anomalous mechanism is characteristic of systems in which the drug is strongly interacting with

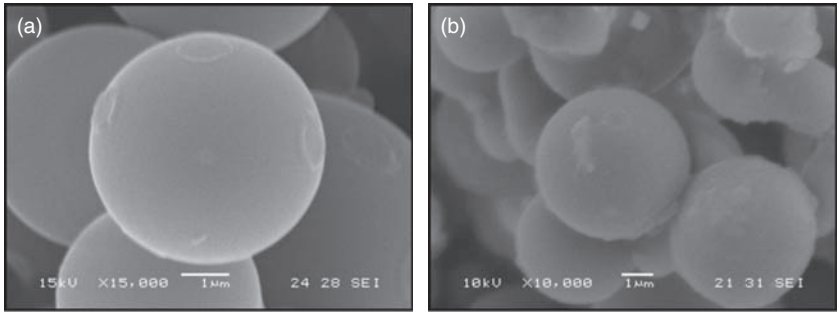

Figure 8. SEM images of GCA hybrid microspheres: (a) before release test in SBF and (b) after 2 weeks of testing in SBF.

the host matrix. According to the FTIR analysis (Figure 2), both systems of microspheres demonstrated the existence of interaction between ASA molecules and the host hybrid matrix; however, from this diffusional analysis (Figure 7), the magnitude of that interaction was evidenced. On the basis of the obtained results, ASA molecules would be more strongly retained into the GCA matrix, which agrees with the nanostructuring features developed in each system. GCA microspheres were characterized for a closer nanostructure (molecular channels defined by a two-dimensional hexagonal structure, Table 1) in comparison to that developed in GDA microparticles (tail-to-tail association of dodecyl chains, Table 1) [14], which would lead to a stronger ASA–matrix interaction and consequently to an anomalous drug-release mechanism.

Figure 8 shows SEM images corresponding to GCA microspheres, before and after testing them in SBF. After 2 weeks of testing, the structural integrity of the microspheres was evidenced, which allowed discarding any possible matrix degradation mechanism. Analogous results were obtained from GDA microspheres.

In vitro ASA-Release Behavior of Composite Calcium Phosphate Bone Cements

Figure 9 depicts the ASA cumulative release profiles corresponding to the composite cements (CPC–GDA and CPC–GCA) in comparison to the one obtained from the control material (CPC–Control). According to the obtained profiles, it is very important to mention that the incorporation of the functionalized hybrid microspheres into the cement systems represented an effective methodology to modify the ASA-release kinetics in comparison to the CPC–Control. More attenuated release profiles

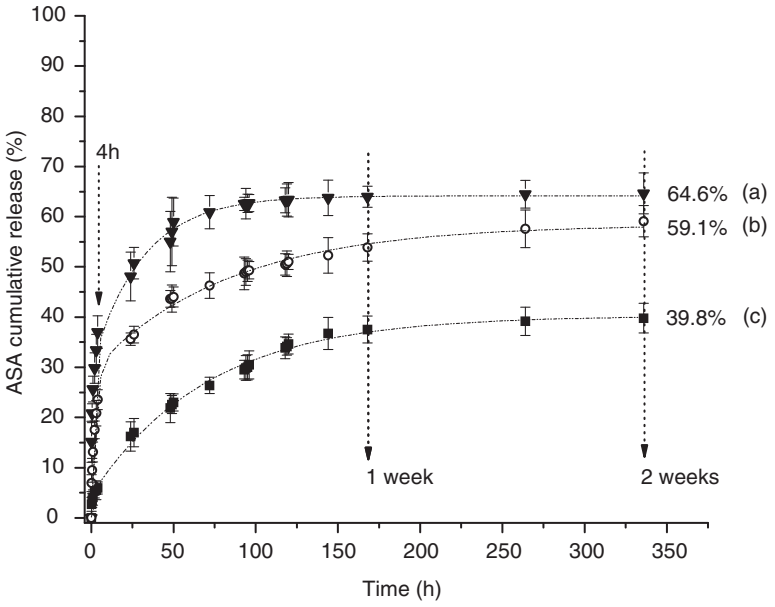

Figure 9. ASA cumulative release profiles obtained from calcium phosphate bone cements: (a) CPC–Control, (b) CPC–GDA, and (c) CPC–GCA.

were obtained from both composite cements, which led us to avoid the initial burst effect characteristic of calcium phosphate bone cements.

A fast ASA release was observed from the profile corresponding to CPC–Control. During the first 4 h of testing, this cement released about 40% of the total ASA content, reaching a value of 62% after 3 days (72 h). After 4 days of testing (96 h), the released amount reached a constant maximum value (64.6%), demonstrating that is the maximum level of drug that can be effectively delivered from CPC–Control after 2 weeks in simulated physiological medium.

On the other hand, according to the profiles corresponding to the composite cements, the CPC–GDA sample led to faster release kinetics in comparison to the CPC–GCA cement. The CPC–GCA formulation allowed us to obtain a strong attenuation of the ASA-release profile (Figure 9(c)). During the first stages (4 h), the CPC–GCA cement released about 6% of the total drug amount, which represented a lower percentage in comparison to the CPC–GDA sample (this sample released about 23% in the same period). After 1 week of testing, the sample CPC–GCA reached its maximum release value, representing about 40% of drug. It is important to notice that this composite cement (CPC–GCA)

led, after 2 weeks, to the same released percentage (within the experimental error) as that obtained from the CPC–Control in only 4 h of testing. This result demonstrated that the incorporation of GCA microspheres allowed strongly attenuating the ASA-release kinetics in comparison to that of a conventional calcium phosphate bone cement containing the drug dispersed into the solid phase.

When the profile corresponding to CPC–GDA cement was analyzed (Figure 9(b)), 54% of ASA was determined after 1 week. In this case, the system reached its maximum value after 11 days (264 h), as observed from the obtained *plateau*. After 2 weeks, the CPC–GDA cement released about the same amount of ASA in comparison to the CPC–Control sample (in the same period) within the experimental error (see error bars). In this way, by incorporating functionalized GDA microspheres, it was possible to moderate the release kinetics in comparison to the control sample (within the first week), allowing provision (after 2 weeks) of the same amount of ASA.

As seen for all prepared cements, it is not possible to release the total amount of ASA incorporated into the solid phases. This could be related to the basic principles involved in the setting and hardening mechanisms of these CPCs. As widely known, these cement systems evolve through dissolution of the reactants (calcium phosphates) and precipitation of the product phase (hydroxyapatite), which grows and leads to the entanglement of the formed crystals. All these events lead to the formation of a microstructure (ceramic matrix) formed by microcrystals and pores which become closer with the immersion time in SBF. This fact leads to a more tortuous material in which part of the incorporated drug is retained into the mentioned microstructure (being, in this way, not available to be released). Some authors have studied the effect of the evolving microstructure of CPCs on the release profiles for different active agents [28]. On these publications, the retention of the incorporated drugs into the cement matrix was mainly attributed to the precipitation of hydroxyapatite crystals on the inner and outer cement surfaces during the release tests, leading to the diminishing of the effective amount of drug available to be delivered.

Figure 10 shows the XRD diffractograms corresponding to the CPC–GDA cement at the beginning of the delivery test (Figure 10(a)) and after 2 weeks immersed in SBF (Figure 10(b)). The evolution of the hardening reaction with the immersion time was easily inferred from the obtained diffraction patterns. After 2 weeks, the cement was composed of low-crystallinity hydroxyapatite. However, after 24 h of hardening (beginning of the delivery test), the sample showed to be composed of low-crystallinity hydroxyapatite as well as of unreacted

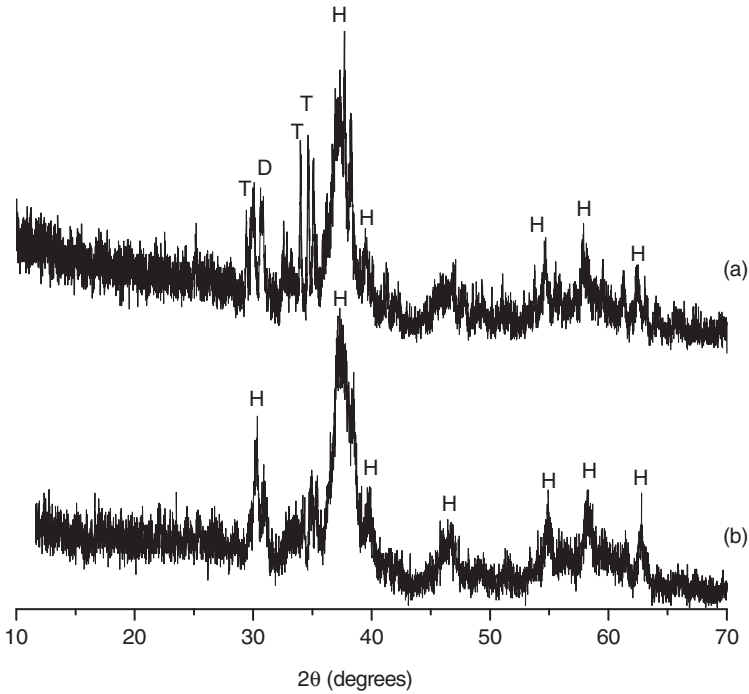

Figure 10. XRD diffractograms corresponding to CPC–GDA composite cement: (a) before release test in SBF and (b) after 2 weeks of testing in SBF. References: H (hydroxyapatite), T (tetracalcium phosphate), and D (dicalcium phosphate anhydrous).

TTCP and DCPA phases. This fact demonstrated that the cement body effectively evolved from calcium phosphate reactants to hydroxyapatite as a consequence of the immersion time in SBF. This result supports the previously mentioned hypothesis: the closer the microstructure of the cement, the lower the amount of ASA released.

Analogous results were obtained from CPC–GCA and CPC–Control samples, before and after testing them in SBF.

In addition to the XRD results, SEM analyses were performed on the fracture surfaces of the cements to evidence the microstructural evolution of the systems. Figure 11 depicts the microstructures corresponding to the CPC–GDA cement at the beginning of the delivery test (Figure 11(a)) and after 2 weeks of testing (Figure 11(b)). Images allowed easily determination of the formation of a closer microstructure as the delivery test proceeded. These results agree with those obtained from XRD analyses and allow justifying why all the prepared cements exhibited a *plateau* in their release profiles. Then, it is not possible to

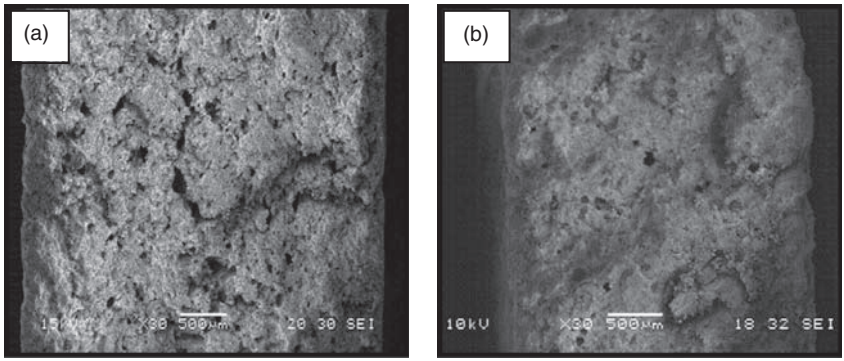

Figure 11. SEM images corresponding to the microstructure of CPC–GDA composite cement: (a) before release test in SBF and (b) after 2 weeks of testing in SBF.

release the entire contents of the incorporated ASA as a consequence of the nature and dynamic behavior of these calcium phosphate bone cements in physiological medium.

In all tested cements, the ASA-delivery mechanism agreed with a diffusional transport of the drug through the micro- and macropores generated into the ceramic matrices. Figure 12 shows the Higuchi analysis (mg of ASA released as a function of time$^{1/2}$) corresponding to the CPC–Control sample. As observed, a linear relationship between the ASA cumulative release and the square root of time exists during the first 4 h of testing. This relationship is not completely linear because the micro- and macroporosity of the cement body continually change as the setting and hardening reactions proceed. According to these results, the CPC–Control cement behaves as an ASA-delivery device, which involves the diffusion of the drug through the calcium phosphate porous matrix, at least during the first 4 h of the delivery test. Analogous results were obtained from CPC–GCA and CPC–GDA samples.

According to all the obtained results, ASA is delivered from the new composite cements (CPC–GDA and CPC–GCA) by a mechanism that involves two stages: (1) the diffusion of the drug through the organic–inorganic matrices of the microspheres (according to a Fickian or anomalous diffusion, depending on the nanostructuring of the microspheres) and (2) the subsequent diffusion of the drug through the ceramic matrix of the hardened cements (through the generated micro- and macropores). However, whatever the operating mechanism, the incorporation of the new functionalized organic–inorganic microdevices into the cements resulted in a viable and effective alternative to achieve

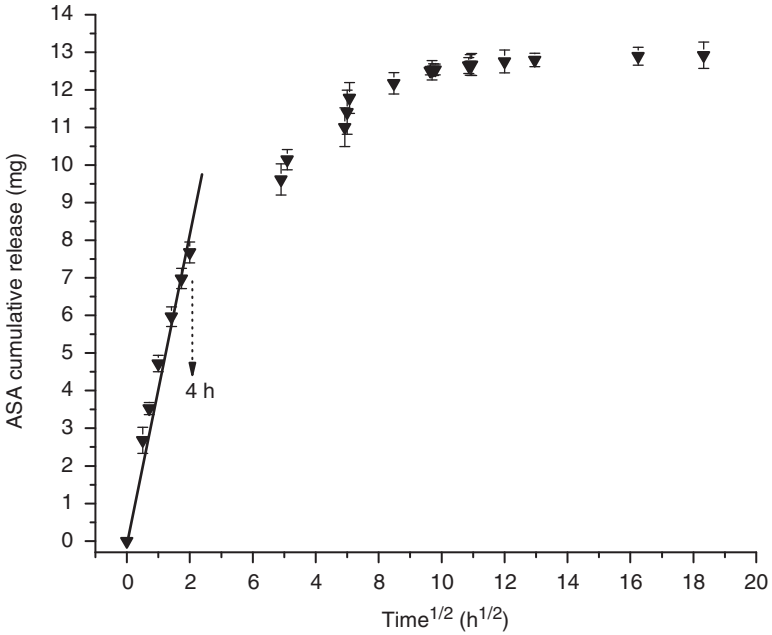

Figure 12. Higuchi plot corresponding to CPC–Control cement.

the availability of the drug into the calcium phosphate systems without modifying the physicochemical properties of the cements, and allowed simultaneously modifying the ASA-delivery profiles in comparison to a conventional cement containing the drug dispersed into the solid phase.

The versatility of the sol–gel method employed to obtain these bridged hybrid systems allowed the development of novel functionalized microdevices characterized by different structuring at molecular level, which depended on the chemical nature of the bridged precursors employed in the synthesis. This nanostructuring mentioned finally determined the behavior of the composite cements as delivery devices. In this way, the significance of employing bridged silsesquioxanes as functional materials (instead of other media of encapsulation) comes from the possibility of selectively modulating the final delivery response of CPCs by tailoring the nanostructuring of these new hybrid microdevices. This can be easily accomplished by choosing the desired chemical structure of the precursors employed in the sol–gel synthesis. This clearly shows the *nanostructure–property* relationship existing for these silica-based bridged hybrids which could potentially be used in bone tissue-related applications.

CONCLUSIONS

The versatility of the sol–gel method allowed us to obtain nanostructured hybrid microspheres *via* self-assembly of organic–inorganic bridged monomers. The architecture reached at molecular level allowed incorporation of ASA as anti-inflammatory model drug. The synthesized microspheres were employed as ASA-delivery systems in simulated physiological medium. The release behavior of the functionalized microspheres was shown to be dependent on the nanostructuring of the hybrid organic–inorganic materials, which can be tailored by selecting the desired chemical structure of the bridged precursors employed in the synthesis.

The incorporation of the functionalized microspheres (regardless of their nanostructuring) into the solid phase of calcium phosphate materials, allowed the development of new composite bone cements with potential use in biomaterials field. The prepared composite cements were characterized by short setting times. The presence of microspheres into the solid phase did not interfere with the dissolution–precipitation kinetics that involves the calcium phosphate reactants. However, the molecular dispersion of ASA into the inorganic matrix led to the modification of the cement properties (longer setting times and lower conversions to hydroxyapatite). The formation of low-crystallinity hydroxyapatite microcrystals on hybrid microspheres during the setting and hardening processes revealed the compatibility between the mentioned crystals (needle-like morphology) and the functionalized microspheres, which was attributed to the presence of Si–OH groups on the hybrid materials. In this way, the incorporation of these new microspheres resulted in a viable and effective alternative to achieve the availability of the drug into the calcium phosphate systems without modifying the physicochemical properties of the cements. The presence of the microspheres into the cement systems allowed us to obtain a change in the ASA-delivery profiles in comparison to a conventional CPC containing the drug dispersed into the solid phase. Depending on the nanostructuring of the employed microspheres, it was possible to selectively modify the delivery behavior of these CPCs in simulated physiological medium. The hybrid microspheres attenuated the rapid ASA release (characteristic of this kind of bone cements) during the first hours of hardening of the systems.

In accordance to all the presented results, these new functionalized nanostructured microspheres could potentially be used as drug carriers and delivery systems into CPCs employed in bone tissue-related drug-delivery applications.

ACKNOWLEDGMENTS

Authors thank the following institutions for providing financial support: National Research Council (CONICET, Argentina), National Agency for the Promotion of Science and Technology (ANPCyT, Argentina), and University of Mar del Plata (Argentina).

REFERENCES

1. Gbureck, U., Vorndran, E., Müller, F.A. and Barralet, J.E. Low Temperature Direct 3D Printed Bioceramics and Biocomposites as Drug Release Matrices, *J. Control. Release*, 2007: **122**: 173–180.
2. Bertazzoni, M., Benini, A., Magnan, B. and Bartolozzi, P. Release of Gentamicin and Vancomycin from Temporary Human Hip Spacers in Two-Stage Revision of Infected Arthroplasty, *J. Antimicrob. Chemother.*, 2004: **53**: 329–334.
3. Castro, C., Sánchez, E., Delgado, A. et al. Ciprofloxacin Implants for Bone Infection. In Vitro-In Vivo Characterization, *J. Control. Release*, 2003: **93**: 341–354.
4. Girod Fullana, S., Ternet, H., Freche, M., Lacout, J.L and Rodriguez F. Controlled Release Properties and Final Macroporosity of a Pectin Microspheres-Calcium Phosphate Composite Bone Cement, *Acta Biomater.*, 2010: **6**: 2294–2300.
5. Lan Levengood, S.K., Polak, S.J., Wheeler, M.B. et al. Multiscale Osteointegration as a New Paradigm for the Design of Calcium Phosphate Scaffolds for Bone Regeneration, *Biomaterials*, 2010: **31**: 3552–3563.
6. Sun, L., Xu, H.H.K., Takagi, S. and Chow, L.C. Fast Setting Calcium Phosphate Cement-Chitosan Composite: Mechanical Properties and Dissolution Rates, *J. Biomater. Appl.*, 2007: **21**: 299–315.
7. Link, D.P., van den Dolder, J., van den Beucken, J.J., Wolke, J.G., Mikos, A.G. and Jansen, J.A. Bone Response and Mechanical Strength of Rabbit Femoral Defects Filled with Injectable CaP Cements Containing TGF-β1 Loaded Gelatin Microparticles, *Biomaterials*, 2008: **29**: 675–682.
8. Klemm, K. Antibiotic Bead Chains, *Clin. Orthop.*, 1993: **295**: 63–76.
9. Iooss, P., Le Ray, A.M., Grimandi, G., Daculsi, G. and Merle, C. A New Injectable Bone Substitute Combining Poly(ε-caprolactone) Microparticles with Biphasic Calcium Phosphate Granules, *Biomaterials*, 2001: **22**: 2785–2794.
10. Mulia, K., Witkamp, G.J., Dawes, G.J.S. et al. Drug Release from PLGA Microspheres Attached to Solids Using Supercritical CO_2, *J. Biomater. Appl.*, 2009: doi:10.1177/0885328209354365.
11. Mori, H., Lanzendörfer, M.G. and Müller, A.H.E. Silsesquioxane-Based Nanoparticles Formed via Hydrolytic Condensation of Organotriethoxysilane Containing Hydroxy Groups, *Macromolecules*, 2004: **37**: 5228–5238.

12. Shea, K.J. and Loy, D.A. Bridged Polysilsesquioxanes: Molecular Engineering of Hybrid Organic-Inorganic Materials, *MRS Bull.*, 2001: **26**: 368–376.
13. Shea, K.J. and Loy, D.A. Bridged Polysilsesquioxanes. Molecular-Engineered Hybrid Organic-Inorganic Materials, *Chem. Mater.*, 2001: **13**: 3306–3319.
14. Romeo, H.E. and Fanovich, M.A. TTCP-DCPA Based Calcium Phosphate Cements Containing Hybrid Microparticles as Drug Carriers, *Key Eng. Mater.*, 2009: **396–398**: 489–492.
15. Romeo, H.E., Fanovich, M.A., Williams, R.J.J., Matejka, L., Plestil, J. and Brus, J. Bridged Silsesquioxanes with Organic Domains Self-Assembled as Functionalized Molecular Channels, *Macromol. Chem. Phys.*, 2007: **208**: 1202–1209.
16. Romeo, H.E., Fanovich, M.A., Williams, R.J.J., Matejka, L., Plestil, J. and Brus, J. Self-Assembly of a Bridged Silsequioxane Containing a Pendant Hydrophobic Chain in the Organic Bridge, *Macromolecules*, 2007: **40**: 1435–1443.
17. Romeo, H.E. and Fanovich, M.A. Synthesis of Tetracalcium Phosphate from Mechanochemically Activated Reactants and Assessment as a Component of Bone Cements, *J. Mater. Sci.: Mater. Med.*, 2008: **19**: 2751–2760.
18. Romeo, H.E., Bueno, P.R. and Fanovich, M.A. Application of Impedance Spectroscopy to Evaluate the Effect of Different Setting Accelerators on the Developed Microstructures of Calcium Phosphate Cements, *J. Mater. Sci.: Mater. Med.*, 2009: **20**: 1619–1627.
19. Bohner, M. and Lemaitre, J. Can Bioactivity be Tested In vitro with SBF Solution?, *Biomaterials*, 2009: **30**: 2175–2179.
20. Colthup, N.B., Daly, L.H. and Wiberley, S.E. (1975). *Introduction to Infrared and Raman Spectroscopy*, New York, Academic Press.
21. Huang, Y., Liu, C.S., Shao, H.F. and Liu, Z.J. Study on the Applied Properties of Tobramycin-Loaded Calcium Phosphate Cement, *Key Eng. Mater.*, 2000: **192**: 853–860.
22. Ginebra, M.P., Rilliard, A., Fernández, E., Elvira, C., San Román, J. and Planell, J.A. Mechanical and Rheological Improvement of a Calcium Phosphate Cement by the Addition of a Polymeric Drug, *J. Biomed. Mater. Res.*, 2001: **57**: 113–118.
23. Hench, L.L. and Wilson, J. (1993). An Introduction to Bioceramics, In: McLaren, M. and Niesz, D.E. (eds), *Advanced Series in Ceramics*, Singapore, World Scientific Publishing Co. Pte. Ltd., Vol. 1, pp. 1–23.
24. Xia, W. and Chang, J. Well-Ordered Mesoporous Bioactive Glasses (MBG): A Promising Bioactive Drug Delivery System, *J. Control. Release*, 2006: **110**: 522–530.
25. Regina Brophy, M. and Deasy, P.B. Application of the Higuchi Model for Drug Release from Dispersed Matrices to Particles of General Shape, *Int. J. Pharm.*, 1987: **37**: 41–47.
26. Sinclair, G.W. and Peppas, N.A. Analysis of non-Fickian Transport in Polymers Using Simplified Exponential Expression, *J. Membr. Sci.*, 1984: **17**: 329–331.

27. Ritger, P.L. and Peppas, N.A. A Simple Equation for Description of Solute Release I. Fickian and non-Fickian Release from Non-swellable Devices in the Form of Slabs, Spheres, Cylinders or Discs, *J. Control. Release*, 1998: **5**: 23–36.
28. Gbureck, U., Vorndran, E. and Barralet, J.E. Vancomycin Release Kinetics from Porous Calcium Phosphate Ceramics Comparing Static and Dynamic Immersion Conditions, *Acta Biomater.*, 2008: **4**: 1480–1486.